Condensed Astatine: Monatomic and Metallic

Andreas Hermann
School of Physics and Astronomy and Centre for Science at Extreme Conditions, University of Edinburgh, Edinburgh, EH9 3JZ, United Kingdom
Department of Chemistry and Chemical Biology, Cornell University, Ithaca, New York 14853, USA

Roald Hoffmann
Department of Chemistry and Chemical Biology, Cornell University, Ithaca, New York 14853, USA

N. W. Ashcroft
Laboratory of Atomic and Solid State Physics, Cornell University, Ithaca, New York 14853, USA
(Received 10 May 2013; published 12 September 2013)

The condensed matter properties of the nominal terminating element of the halogen group with atomic number 85, astatine, are as yet unknown. In the intervening more than 70 years since its discovery significant advances have been made in substrate cooling and the other techniques necessary for the production of the element to the point where we might now enquire about the key properties astatine might have if it attained a condensed phase. This subject is addressed here using density functional theory and structural selection methods, with an accounting for relativistic physics that is essential. Condensed astatine is predicted to be quite different in fascinating ways from iodine, being already at 1 atm a metal, and monatomic at that, and possibly a superconductor (as is dense iodine).

DOI: 10.1103/PhysRevLett.111.116404 PACS numbers: 71.20.−b, 71.15.Mb, 71.15.Rf

When examining Mendeleev's enduring periodic array with respect to the physical attributes of the condensed phase of an element, a very noticeable vacancy can be observed. The quite evident gap occurs immediately below iodine, at the atomic location assigned to astatine. This, the heaviest named element in the halogen group with atomic number 85, and electronic configuration $[\mathrm{Xe}]4f^{14}5d^{10}6s^{2}6p^{5}$, was isolated in 1940 by Corson, MacKenzie, and Segrè [1] through bombardment of a bismuth substrate with α particles. It was aptly named by its discoverers (the name derives from *astatos* meaning in Greek "unstable") for indeed astatine lacks any stable isotopes [2]. Quite recently, group 17 has been formally extended through the single-atom production of element 117 [3].

The half-lives $t_{1/2}$ of the unstable astatine isotopes, which span the mass range from ^{193}At to ^{223}At, range from 125 ns for ^{213}At to 8.1 h for ^{210}At [4]. The second longest living isotope, ^{211}At, with $t_{1/2} = 7.2$ h, is used as an α emitter in radionuclide therapy [5,6]. It can be produced at a rate of 1.5×10^{12} atoms/h, by accelerating a 1 μA current of α particles onto a ^{209}Bi target in a cyclotron [7]. Hence, it should be possible to gather a sufficient quantity of astatine atoms to form a condensed state, as was evidently achieved by Corson *et al.* Yet to be determined is (i) whether astatine as a collision product can be captured to form a solid film on a suitable substrate, and (ii) whether the effects of significant radiation emitted upon decay of the atoms (α and β^{+} for ^{210}At and ^{211}At) might be ameliorated by sufficient steady external cooling to prevent deterioration of a macroscopic sample of astatine.

Little is known of the physical and chemical properties of condensed astatine [8], and an examination of the available evidence [9] gives no direct evidence of those properties. It appears that an amount of the element sufficient to examine the relevant condensed state properties has not yet been made. However, some of the chemistry of astatine has been inferred from experiments on ion beams [10] and very dilute solutions [1], and that chemistry has been compared to properties of the other halogens. In fact, estimates of the boiling point of astatine [11], its cohesive energy [12], as well as a qualitative argument for the solid being metallic have been made [13]. Thus the study of astatine will not only put the properties of the lighter halogen analogues into perspective, but also provide the link to understanding the above-mentioned, recently synthesized element E117.

Given this motivation, we report here relativistic density functional theory (DFT) calculations addressing the physical nature of the condensed state of astatine. We predict it to be metallic at one atmosphere, and also beyond. This sets it quite apart from the lighter halogens, whose high-pressure properties we must also discuss as an important calibration for what follows. As will become evident, inclusion of spin-orbit and fluctuating multipole (or dispersion) interactions is crucial for a correct description of astatine's condensed state.

We preface our treatment of condensed astatine with a brief summary of the key structural properties of its halogen forerunners. At atmospheric pressures, all solid

halogens are molecular crystals, composed of halogen dimers. Experimentally, it is found that as the halogens become more massive, the atomic separations in the isolated dimers increase monotonically, and the binding energies D_e and vibrational frequencies ω_e also decrease accordingly [see the Supplemental Material (SM) [14], and references therein for details on the molecular properties of the halogens]. For the isolated At_2 dimer, only computational results are known to date, but the trends have been in line with those of the lighter halogens.

For chlorine, bromine, and iodine, scalar relativistic DFT calculations with the Perdew-Burke-Ernzerhof exchange-correlation functional [15] describe the structural and vibrational properties of the respective dimers very well (see the SM [14] for a comparison of plane-wave calculations with the VASP package [16,17] and atom-centered basis set calculations [18–20] with the GAUSSIAN09 program suite [21]). Mean atomic separations are then within 1% of the experimental values, and the vibron frequencies deviate only by about 3% or less from experiment. Atomic and molecular dipole polarizabilities also agree well with high-level quantum chemical calculations, which used the coupled-cluster method (with perturbative treatment of triple excitations) and also included spin-orbit coupling [22]. For the astatine dimer, spin-orbit coupling plays an important role: only upon inclusion of spin-orbit effects are both the atomic separations (1% too long) and vibron frequencies (6% too small) close to fully relativistic coupled cluster results. Scalar relativistic DFT, on the other hand, can lead to significant overbinding of the dimers of all halogens.

From the known atomic or molecular dipole polarizabilities, we can estimate the atomic densities required to form metallic solids as a consequence of an emerging polarization catastrophe [23,24]. In this respect the Goldhammer-Herzfeld approach to metallization has proven itself useful [25]. As these polarizabilities increase monotonically proceeding down the halogen group, the estimated compressions necessary for metallization decrease monotonically (to about $V_0/V = 1.87$ for solid iodine, compared to the experimental metallization at $V_0/V = 1.45$). Hence, we may expect the ground state of astatine to be a weakly bound molecular or indeed even an atomic crystal, and to either be metallic or to require comparatively little additional densification via external pressure to induce metallization.

The known halogens fluorine, chlorine, bromine, and iodine all share similar crystalline state structure types at atmospheric pressure: their molecular dimer units are arranged in a herringbonelike packing in two-dimensional layers, and these layers are weakly bound to each other, presumably by dispersion interactions. The ground state structure of fluorine is a monoclinic crystal of $C2/c$ symmetry [26], and those of chlorine, bromine, and iodine are all orthorhombic crystals of $Cmca$ symmetry, with $Z = 8$ atoms per unit cell [27]. All of these paired molecular

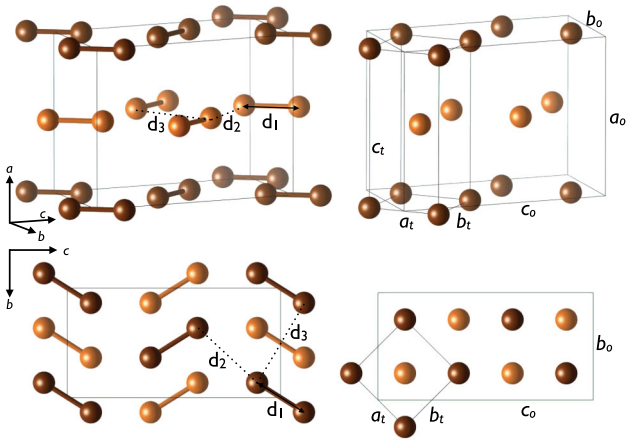

FIG. 1 (color online). Left: Molecular $Cmca$ phase of the halogens, with shortest atomic distances indicated. Right: the unit cell of the atomic $I4/mmm$ phase (lattice a_t, b_t, c_t) in relation to the $Cmca$ unit cell (lattice a_o, b_o, c_o). Side-on and top views are given, respectively. Different shades denote atoms in different layers.

crystals are insulating at atmospheric pressure, but metallic states can be reached through application of external pressure. This property makes the group 17 halogens highly intriguing comparative model systems for the elusive metallization of group 1 hydrogen [28], and their structural and electronic properties under pressure have been studied widely, both through extensive computation [29] and experiment [30–35].

In Fig. 1, the ground-state $Cmca$ structure is presented, this indicating the intramolecular atomic separation d_1, and the two shortest intermolecular separations d_2 and d_3. In this structure, the layers of halogen dimers are stacked along the crystalline a axis. As the herringbone layers are largely held together by dispersion interactions, local or semilocal DFT functionals overestimate the distances between these layers. If dispersion interactions are accounted for (there are several ways to accomplish this, see, e.g., Refs. [36,37]), the theoretically predicted crystal structures of the halogens are then in very satisfactory agreement with experiment (see the SM [14] for details).

At higher pressures, the intermolecular separations between the halogen dimers in their crystals steadily decrease, until "equalization" is reached, meaning simply that the intra- and shortest intermolecular separations eventually equalize [38]. Importantly, ground-state metallization seems to set in consistently *before* equalization is reached (for all halogen elements [30]) resulting in paired but metallic states, a feature also projected for dense hydrogen (and indeed this is in agreement with theoretical predictions on metallic hydrogen structures [39]). Consistent with this, the DFT band gap of the halogens (which probably underestimates the actual band gap) closes while the structures are still molecular: at $P = 140$ GPa for chlorine (the atomic phase is reached at $P = 180$ GPa), $P = 45$ GPa for bromine (atomic

phase at $P = 60$ GPa), and $P = 16$ GPa for iodine (atomic phase at $P = 21$ GPa). The *Cmca* structure in chlorine, bromine, and iodine is, as pressure is increased, followed by the structural sequence body-centered orthorhombic (bco, space group *Immm*), body-centered tetragonal (bct, $I4/mmm$), and face-centered cubic (fcc, Fm-3m). An incommensurate modulated structure is found as an intermediate between the *Cmca* and *Immm* structures [34]. The pressures needed to attain an atomic phase decrease rapidly for the heavier halogens. And since high-pressure phases of each halogen are found to be stable at lower pressures in heavier halogens, plausible candidates for astatine's ground-state structure (besides the molecular *Cmca* phase) are therefore the atomic phases just introduced.

For the two heaviest halogens, iodine and astatine, relativistic effects (in particular spin-orbit coupling) are *a priori* expected to play an important role in the ground-state energetics, since they scale roughly with Z^2, Z being the nuclear charge [40–42]. We therefore performed solid-state DFT calculations, both at the scalar-relativistic and spin-orbit level of theory, for iodine and astatine. Scalar-relativistic effects are included in the construction of the projector augmented wave (PAW) data sets [17], and spin-orbit effects are evaluated in second-order approximation on a radial grid within the PAW spheres [43]. For the ground but extended state of astatine, we initially assumed the *Cmca* structure. Figure 2 compares the structural properties of astatine and iodine as a function of pressure. The transition from a molecular to an atomic solid can be intuitively visualized through the use of an equalization index ζ [38]: $\zeta(P) = 1 - (d_2 - d_1)_P/(d_2 - d_1)_0$ at each pressure P, where d_1 and d_2 denote the shortest intra- and intermolecular distances, respectively; and $(\ldots)_P$ refers to those values taken at pressure P. By its very definition $\zeta = 0$ at atmospheric pressure, and $\zeta = 1$ when the atomic state is reached.

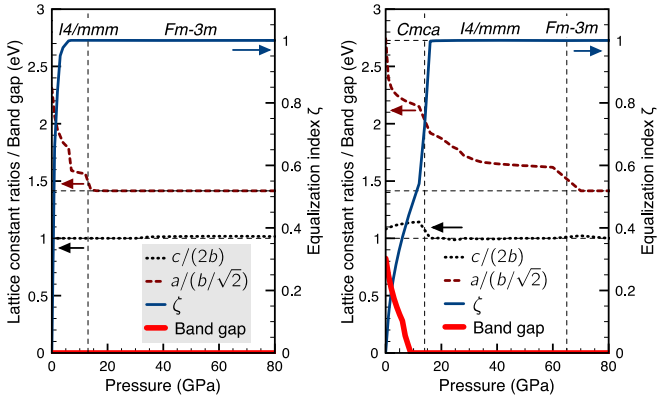

FIG. 2 (color online). Structural and electronic properties of static crystalline astatine (left) and iodine (right), as calculated from spin-orbit coupling DFT calculations. The left-hand axis refers to lattice constant ratios (dimensionless) and band gaps (eV). The right-hand axis gives the computed equalization index (dimensionless). As remarked in the text, condensed astatine is metallic at all pressures considered here; it has no band gap. Note that the equalization index ζ of astatine is not identically 1 at all pressures: when starting the structural optimization from the *Cmca* phase at $P = 1$ atm, the shortest At-At distances d_1 and d_2 differ only by about 0.04%—a difference entirely within the numerical accuracy of the optimization algorithm.

For iodine, the influence of spin-orbit coupling becomes quite noticeable at high pressures, as the transition pressure from the *Cmca* to the $I4/mmm$ structure changes from 21 GPa at the scalar-relativistic level to 16 GPa at the spin-orbit level of theory. Even more pronounced is the change in the pressure associated with the transition to the fcc structure: 32 GPa from scalar-relativistic DFT, and 65 GPa from spin-orbit DFT calculations. Spin-orbit effects are most relevant near the nuclei where large potential gradients are found; with significant external pressure, a valence electron's probability to be located near a nucleus is expected to increase, and hence also the influence of spin-orbit effects.

For astatine, scalar-relativistic DFT calculations predict a *molecular* ground state at atmospheric pressure, with a transition to the atomic $I4/mmm$ structure at $P = 15$ GPa (or $V_0/V \sim 1.7$, see the SM [14]). This is in fact not very different from the case for iodine. Moreover, DFT predicts a band gap for astatine of 0.68 eV at atmospheric pressure, and band gap closure at $P = 9$ GPa. However, upon inclusion of spin-orbit effects, the situation changes markedly; the ground state of astatine at atmospheric pressure is now found to be the atomic, non-molecular $I4/mmm$ structure. Accordingly, condensed astatine is now predicted to be an atomic and metallic solid. At $P = 13$ GPa, the fcc structure is taken up (see Fig. 2). Spin-orbit effects thus qualitatively influence the calculated properties of crystalline astatine. The additional inclusion of dispersion interactions in the form of Grimme's correction [37] (which gives reasonable agreement for solid-state structures of other simple metals, see the SM [14]) results in an fcc structure for solid astatine, by reducing the c/a ratio of the $I4/mmm$ structure to $c/a = \sqrt{2}$ (with $a = 3.81$ Å). The atomic and metallic (see below) character of astatine is thus confirmed. Moreover, the lattice binding energy of $E_b = 1.62$ eV/atom agrees very well with the experimental estimate of the sublimation enthalpy, $\Delta H_f = 1.53 \pm 0.26$ eV/atom, obtained from surface adsorption measurements of single astatine atoms [12]. We therefore suggest that the element astatine will then be the only halogen that does not have a molecular ground state at $P = 1$ atm, and also the only halogen that is metallic at all higher pressures.

While the large static dipole polarizability of astatine (43 . . . 45.6 a.u. [44]) explains the significant influence of dispersion interactions on the ground-state structure, it also suggests that treatment of these interactions beyond the simple pair-potential approach of the Grimme correction could be instructive, for instance by taking into account screening effects of the eventual metallic environment [45,46] as well as the consideration of higher-order terms,

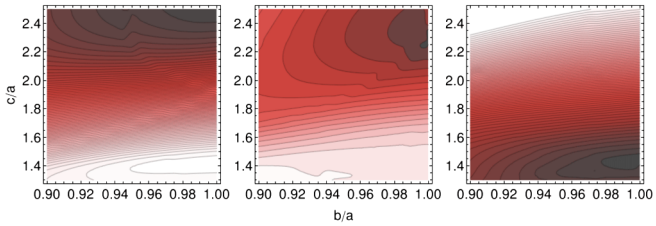

FIG. 3 (color online). Calculated static ground-state enthalpy surface for atomic astatine in the *Immm* space group at $P = 1$ atm: left for scalar-relativistic DFT, middle for spin-orbit DFT, right for spin-orbit DFT-D2 with dispersion correction. Enthalpies are relative to the global minimum and per atom, with isoenergetic lines 10 meV/atom apart. Dark (light) colors refer to lower (higher) enthalpies.

such as the three-body interactions of the Axilrod-Teller type [47]. From the $E(V)$ equation of state we obtain a Debye temperature of $T_D = 195$ K for ^{210}At, which compares with the Debye temperature range of 162 K we obtain for iodine. We thus would not expect an unusually low melting point of solid astatine.

A geometry optimization starting from the molecular *Cmca* phase is restricted by symmetry, as general bco structures are not attainable. But we can sample the ground state energy surface of astatine explicitly for atomic bco structures as a function of the lattice ratios c/a and b/a. As shown in Fig. 3, on the scalar-relativistic level at $P = 1$ atm, we find the minimum (in this bco sub-space of crystal structures) to have an exceedingly large c/a ratio (about 2.6), while for spin-orbit calculations at $P = 1$ atm, the global minimum is indeed of $I4/mmm$ symmetry (albeit again with a very large c/a ratio of about 2.3), and the additional inclusion of dispersion interactions confirms the fcc ground state structure.

It is quite pertinent to ask what other simple ground-state atomic structures could arise. Studies of the ground-state properties of astatine in a variety of simple atomic structures are listed in the SM [14]; relativity in the form of spin-orbit coupling again plays an important role for the energetic orderings of these structures, but more importantly they can all be ruled as structural alternatives at atmospheric pressure on energetic grounds. We also performed a comprehensive structure search at $P = 1$ atm (with $Z = 4$ astatine atoms in the unit cell, and including spin-orbit coupling, but no dispersion corrections) with a random set of initial structures, and using evolutionary algorithms to find candidates for the ground-state structure [48]. This search independently confirmed the $I4/mmm$ structure as the ground state for condensed crystalline astatine.

As expected, the electronic properties of astatine will depend as much on the level of theory as on chosen structural properties. In fact, scalar-relativistic DFT predicts crystalline astatine to be a semiconducting molecular solid, while the inclusion of spin-orbit and dispersion effects results in a quite metallic ground state. The calculated band structures and electronic densities of states (DOS) of the respective ground-state structures are shown in Fig. 4.

By way of conclusion, we propose that at $P = 1$ atm the element astatine, discovered more than 70 years ago, will take up not a molecular but an atomic face-centered cubic crystal structure in the condensed state, and it will be a metal. Spin-orbit effects play a quite crucial role in correctly describing the structural and electronic properties of astatine (they play a more minor role in its lighter homologue iodine), as do dispersion interactions. A trend for increasingly smaller metallization pressures down the halogen group culminates in a metallic ground state for astatine but now at atmospheric pressure.

Perhaps the most striking feature of Fig. 4 (right) is the scale of the electronic density of states at the Fermi level: 0.13 states/eV/e, compared to 0.10 states/eV/e for metallic and superconducting iodine at $P = 30$ GPa in the *Immm* phase. It is then very likely that astatine will follow theoretical suit, though because of ever present radiative heating, establishing this experimentally may well pose some interesting challenges. It will be of considerable interest to examine the character and scale of effective ion-ion interactions in a metallic phase of astatine especially with respect to the possibility of the occurrence of a fairly low melting point (recalling that mercury is also a case where relativistic effects are of some importance [49]).

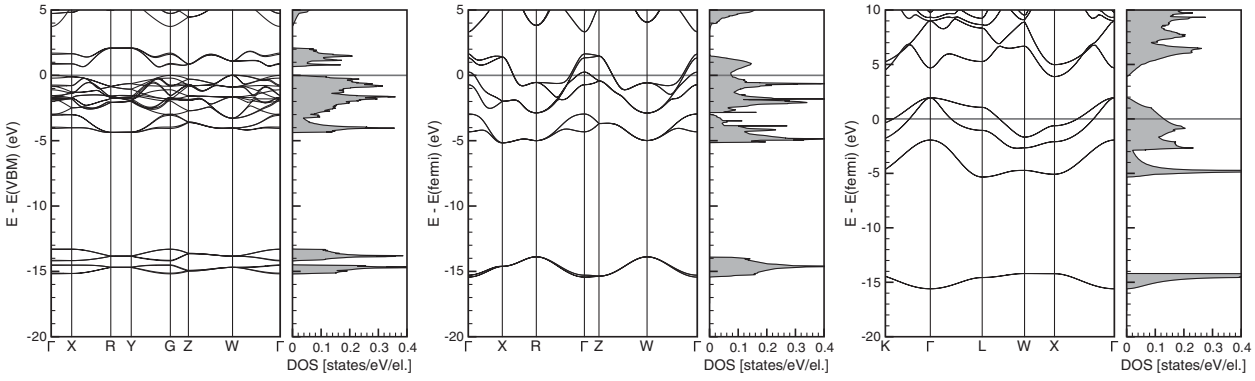

FIG. 4. Band structure and DOS of At, various level of theory. Left: scalar-relativistic DFT (*Cmca* structure, $Z = 4$), middle: including spin-orbit effects ($I4/mmm$ structure, $Z = 2$), right: also including dispersion interactions (Fm-3m structure, $Z = 1$).

A. H. wishes to thank Ralf Tonner for supplying the astatine $D2$ parameters, Heinz Gäggeler for a reprint of their work on astatine, and Peter Schwerdtfeger for piquing his interest in (super)heavy elements. The authors acknowledge the inspiration gained for this study from the work of their late colleague, Dale Corson. This work was supported by the National Science Foundation through Grants No. DMR-0907425 and No. CHE-0910623, and also by EFree, an Energy Frontier Research Center funded by the U.S. Department of Energy (Award No. DESC0001057 at Cornell). Computational resources provided by the Cornell NanoScale Facility (supported by the National Science Foundation through Grant No. ECS-0335765) are gratefully acknowledged.

[1] D. R. Corson, K. R. MacKenzie, and E. Segrè, Phys. Rev. **58**, 672 (1940).
[2] D. R. Corson, K. R. MacKenzie, and E. Segrè, Nature (London) **159**, 24 (1947).
[3] Yu. Ts. Oganessian *et al.*, Phys. Rev. Lett. **104**, 142502 (2010).
[4] R. B. Firestone and S. Y. Frank Chu, *Table of Isotopes* (Wiley-Interscience, New York, 1998), 8th ed.
[5] M. R. McDevitt, G. Sgouros, R. D. Finn, J. L. Humm, J. G. Jurcic, S. M. Larson, and D. A. Scheinberg, Eur. J. Nucl. Med. **25**, 1341 (1998).
[6] M. R. Zalutsky, P. K. Garg, H. S. Friedman, and D. D. Bigner, Proc. Natl. Acad. Sci. U.S.A. **86**, 7149 (1989).
[7] R. H. Larsen, B. W. Wieland, and M. R. Zalutsky, Appl. Radiat. Isot. **47**, 135 (1996).
[8] D. S. Wilbur, Nat. Chem. **5**, 246 (2013).
[9] L. Vasáros and K. Berei in *Gmelin Handbook of Inorganic Chemistry* (Springer, Berlin, 1985), 8th ed., pp. 107–128.
[10] S. Rothe *et al.*, Nat. Commun. **4**, 1835 (2013).
[11] K. Otozai and N. Takahashi, Radiochim. Acta **31**, 201 (1982).
[12] A. Serov *et al.*, Radiochim. Acta **99**, 593 (2011).
[13] S. Siekierski and J. Burgess, *Concise Chemistry of the Elements* (Horwood, Chichester, 2002), pp. 122–123.
[14] See Supplemental Material at http://link.aps.org/supplemental/10.1103/PhysRevLett.111.116404 for structural and electronic properties of the lighter halogen dimers and solid state structures.
[15] J. P. Perdew, K. Burke, and M. Ernzerhof, Phys. Rev. Lett. **77**, 3865 (1996).
[16] G. Kresse and J. Furthmüller, Phys. Rev. B **54**, 11 169 (1996).
[17] G. Kresse and D. Joubert, Phys. Rev. B **59**, 1758 (1999).
[18] T. H. Dunning, Jr., J. Chem. Phys. **90**, 1007 (1989).
[19] A. K. Wilson, D. E. Woon, K. A. Peterson, and T. H. Dunning, J. Chem. Phys. **110**, 7667 (1999).
[20] K. A. Peterson, D. Figgen, E. Goll, H. Stoll, and M. Dolg, J. Chem. Phys. **119**, 11 113 (2003).
[21] M. J. Frisch *et al.*, GAUSSIAN 09, revision A.02, Gaussian, Inc., Wallingford, CT (2009).
[22] M. Dolg, Mol. Phys. **88**, 1645 (1996).
[23] D. A. Goldhammer, *Dispersion Und Absorption Des Lichtes* (Teubner Verlag, Leipzig, 1913).
[24] K. F. Herzfeld, Phys. Rev. **29**, 701 (1927).
[25] P. P. Edwards and M. J. Sienko, Acc. Chem. Res. **15**, 87 (1982).
[26] L. Pauling, I. Keaveny, and A. B. Robinson, J. Solid State Chem. **2**, 225 (1970).
[27] P. M. Harris, E. Mack, Jr., and F. C. Blake, J. Am. Chem. Soc. **50**, 1583 (1928); B. Vonnegut and B. E. Warren, J. Am. Chem. Soc. **58**, 2459 (1936); R. L. Collin, Acta Crystallogr. **5**, 431 (1952); B. M. Powell, K. M. Heal, and B. H. Torrie, Mol. Phys. **53**, 929 (1984); R. M. Ibberson, O. Moze, and C. Petrillo, Mol. Phys. **76**, 395 (1992).
[28] E. Wigner and H. B. Huntington, J. Chem. Phys. **3**, 764 (1935).
[29] M. S. Miao, V. E. Van Doren, and J. L. Martins, Phys. Rev. B **68**, 094106 (2003); D. Duan, X. Jin, Y. Ma, T. Cui, B. Liu, and G. Zou, Phys. Rev. B **79**, 064518 (2009); D. Duan, Y. Liu, Y. Ma, Z. Liu, T. Cui, B. Liu, and G. Zou, Phys. Rev. B **76**, 104113 (2007); D. Duan, X. Meng, F. Tian, C. Chen, L. Wang, Y. Ma, T. Cui, B. Liu, Z. He, and G. Zou, J. Phys. Condens. Matter **22**, 015702 (2010); P. Li, G. Gao, and Y. Ma, J. Chem. Phys. **137**, 064502 (2012).
[30] H. Fujihisa, Y. Fujii, K. Takemura, and O. Shimomura, J. Phys. Chem. Solids **56**, 1439 (1995).
[31] Y. Fujii, K. Hase, Y. Ohishi, N. Hamaya, and A. Onodera, Solid State Commun. **59**, 85 (1986).
[32] Y. Fujii, K. Hase, N. Hamaya, Y. Ohishi, A. Onodera, O. Shimomura, and K. Takemura, Phys. Rev. Lett. **58**, 796 (1987).
[33] T. Kenichi, S. Kyoko, F. Hiroshi, and O. Mitsuko, Nature (London) **423**, 971 (2003).
[34] T. Kume, T. Hiraoka, Y. Ohya, S. Sasaki, and H. Shimizu, Phys. Rev. Lett. **94**, 065506 (2005).
[35] K. Takemura, S. Minomura, O. Shimomura, and Y. Fujii, Phys. Rev. Lett. **45**, 1881 (1980).
[36] F. Ortmann, F. Bechstedt, and W. G. Schmidt, Phys. Rev. B **73**, 205101 (2006); M. Dion, H. Rydberg, E. Schroder, D. C. Langreth, and B. I. Lundqvist, Phys. Rev. Lett. **92**, 246401 (2004); G. Román-Pérez and J. Soler, Phys. Rev. Lett. **103**, 096102 (2009); J. Klimeš, D. Bowler, and A. Michaelides, Phys. Rev. B **83**, 195131 (2011); A. Tkatchenko and M. Scheffler, Phys. Rev. Lett. **102**, 073005 (2009).
[37] S. Grimme, J. Comput. Chem. **27**, 1787 (2006).
[38] V. Labet, P. Gonzalez-Morelos, R. Hoffmann, and N. W. Ashcroft, J. Chem. Phys. **136**, 074501 (2012).
[39] C. J. Pickard and R. J. Needs, Nat. Phys. **3**, 473 (2007).
[40] J. Dehmer, Phys. Rev. A **7**, 4 (1973).
[41] W. H. E. Schwarz, E. M. van Wezenbeek, E. J. Baerends, and J. G. Snijders, J. Phys. B **22**, 1515 (1989).
[42] A. Hermann, J. Furthmüller, H. W. Gäggeler, and P. Schwerdtfeger, Phys. Rev. B **82**, 155116 (2010).
[43] Y.-S. Kim, K. Hummer, and G. Kresse, Phys. Rev. B **80**, 035203 (2009).
[44] P. Schwerdtfeger, http://ctcp.massey.ac.nz/dipole-polarizabilities (2011).
[45] J. J. Rehr, E. Zaremba, and W. Kohn, Phys. Rev. B **12**, 2062 (1975).
[46] A. C. Maggs and N. W. Ashcroft, Phys. Rev. Lett. **59**, 113 (1987).
[47] B. M. Axilrod and E. Teller, J. Chem. Phys. **11**, 299 (1943).
[48] D. C. Lonie and E. Zurek, Comput. Phys. Commun. **182**, 372 (2011).
[49] F. Calvo, E. Pahl, M. Wormit, and P. Schwerdtfeger. Angew. Chem., Int. Ed. **52**, 7583 (2013).